

Removing Bias from Discrete Time Models Based on Finite Interval Response Data

Myles L. Baker* and D. Lewis Mingori†

University of California, Los Angeles, Los Angeles, California 90095

Modern off-line system identification methods necessarily form a system realization using a finite amount of data. The models constructed are usually of an order smaller than the actual order of the physical system because it is not practical to model the relatively unimportant states. A method is presented to improve the selection of the important states and the model order in system identification methods based on generalized Hankel matrices. When forming a reduced-order model, it is critical to be able to accurately identify the important states and to select the appropriate model order. Some currently popular methods implicitly contain a frequency weighting that comes from the use of a finite time interval of data in the identification. A method is presented to remove this implicit bias, and excellent results are obtained, even when the response data used span only a fraction of a cycle of the dominant frequency.

Introduction

THIS paper is concerned with the problem of constructing a discrete time state-space model of a system of unknown order based on knowledge of the unit pulse response (i.e., Markov parameters) over a finite time interval. The focus is on reducing the errors introduced by using a finite time interval of pulse response data to construct a state-space model. The results are also of interest whenever a low-order (reduced) model is constructed using a small amount of data. A procedure is proposed that has much in common with the Eigensystem Realization Algorithm (ERA)^{1,2} but differs in the steps in which the model order is determined and the state-space matrices are constructed. The new procedure produces a model that is internally balanced on the semi-infinite interval $0 \leq t \leq \infty$. It has been used very successfully even when the available response data span only a fraction of an oscillation of the dominant frequency.

Consider a discrete time dynamic system described by the state-space equations

$$x(k+1) = Ax(k) + Bu(k) \quad (1)$$

$$y(k) = Cx(k) \quad (2)$$

where x is a state vector of length n , u is an input vector of length m , and y is an output vector of length p . For zero initial conditions, the response of the system can be expressed as

$$y(i) = \sum_{k=1}^i Y(k)u(i-k) \quad (3)$$

$$Y(k) = CA^{k-1}B \quad (4)$$

The quantities $Y(k)$ are known as the Markov parameters, and they describe the unit pulse response of the system. [Consider Eq. (3) and let $u(k) = 1$ for $k = 0$ and 0 for $k > 0$.] The Markov parameters could in principle be determined by conducting an experiment in which the actual input to the system was a unit pulse. In practice, however, it is typical to use any of several methods by which Markov

parameters can be estimated from experimental data even if the input is not a unit pulse. It is not our objective here to address the question of how the unit pulse response data are obtained. This is considered, for example, in Refs. 3–5. Instead, we consider what happens if accurate (noise-free) values for the $Y(k)$ are known for some finite number of k , and we wish to use these data to generate a state-space model of the system.

In Refs. 1 and 2, the authors describe a procedure called the ERA for constructing a state-space model from known Markov parameters. To illustrate the effects of using a finite amount of data, first consider the implementation of the ERA. The first step in this procedure is to introduce a generalized Hankel matrix defined as

$$H_{rs}(k) = \begin{bmatrix} CA^{k+j_0+t_0}B & CA^{k+j_0+t_1}B & \dots & CA^{k+j_0+t_{s-1}}B \\ CA^{k+j_1+t_0}B & CA^{k+j_1+t_1}B & \dots & CA^{k+j_1+t_{s-1}}B \\ \vdots & \vdots & \ddots & \vdots \\ CA^{k+j_{r-1}+t_0}B & CA^{k+j_{r-1}+t_1}B & \dots & CA^{k+j_{r-1}+t_{s-1}}B \end{bmatrix} \quad (5)$$

where r, s, t_i ($i = 0 \dots s-1$), and j_i ($i = 0 \dots r-1$) are arbitrary integers. $H_{rs}(k)$ can be expressed in the form

$$H_{rs}(k) = V_r A^k W_s \quad (6)$$

where

$$V_r = \begin{bmatrix} CA^{j_0} \\ CA^{j_1} \\ \vdots \\ CA^{j_{r-1}} \end{bmatrix} \quad W_s = [A^{t_0}B \quad A^{t_1}B \quad \dots \quad A^{t_{s-1}}B] \quad (7)$$

The Hankel matrix $H_{rs}(0)$ may be constructed using the Markov parameters that are presumed known from the pulse response. This step involves choosing values for $(j_0, \dots, j_{r-1}, t_0, \dots, t_{s-1})$ and making a decision about the size of $H_{rs}(0)$. $H_{rs}(0)$ must be small enough so that it can be constructed using only the known Markov parameters and also so that the computational cost associated with the subsequent singular-value decomposition and matrix operations is not prohibitive. Once $H_{rs}(0)$ is constructed, a singular-value decomposition^{6,7} leads to the representation of $H_{rs}(0)$ as

$$H_{rs}(0) = PDQ^T \quad (8)$$

where P is $rp \times n$ and unitary, Q is $ms \times n$ and unitary, D is $n \times n$ and diagonal, and $n = \text{rank}[H_{rs}(0)]$. In this context, the integer n

Presented as Paper 94-3640 at the AIAA Guidance, Navigation, and Control Conference, Scottsdale, AZ, Aug. 1–3, 1994; received Aug. 11, 1994; revision received Jan. 17, 1996; accepted for publication March 18, 1996. Copyright © 1996 by the American Institute of Aeronautics and Astronautics, Inc. All rights reserved.

*Graduate Student, Mechanical, Aerospace, and Nuclear Engineering Department. Student Member AIAA.

†Professor, Mechanical, Aerospace, and Nuclear Engineering Department. Associate Fellow AIAA.

represents the maximum possible dimension of the state-space system identified rather than the true order of the system. The singular values of $H_{rs}(0)$ are arranged in descending order on the diagonal of D . The matrices P , D , and Q may be partitioned such that

$$H_{rs}(0) = [P_\ell \quad P_{n-\ell}] \begin{bmatrix} D_\ell & 0 \\ 0 & D_{n-\ell} \end{bmatrix} \begin{bmatrix} Q_\ell^T \\ Q_{n-\ell}^T \end{bmatrix} \quad (9)$$

$$= P_\ell D_\ell Q_\ell^T + P_{n-\ell} D_{n-\ell} Q_{n-\ell}^T$$

This partitioning is guided by the sizes of the singular values of $D_{n-\ell}$ relative to those of D_ℓ . If the diagonal entries in $D_{n-\ell}$ are sufficiently small compared with those of D_ℓ , it can be argued that the second term in (9) may be neglected, leading to

$$H_{rs}(0) \cong P_\ell D_\ell Q_\ell^T \quad (10)$$

An ℓ th-order system representation (A_ℓ , B_ℓ , C_ℓ) that satisfies Eq. (5) within the truncation approximation can be constructed using

$$A_\ell = D_\ell^{-\frac{1}{2}} P_\ell^T H_{rs}(1) Q_\ell D_\ell^{-\frac{1}{2}} \quad (11)$$

$$B_\ell = D_\ell^{\frac{1}{2}} Q_\ell^T E_m \quad C_\ell = E_p^T P_\ell D_\ell^{\frac{1}{2}}$$

where E_m consists of the first m rows of an ms -order identity matrix and E_p consists of the first p rows of an rp -order identity matrix. This is equivalent to forming an n th-order model (A_n , B_n , C_n), partitioning the matrices such that

$$A_n = \begin{bmatrix} A_\ell & A_{\ell, n-\ell} \\ A_{n-\ell, \ell} & A_{n-\ell} \end{bmatrix} \quad B_n = \begin{bmatrix} B_\ell \\ B_{n-\ell} \end{bmatrix} \quad (12)$$

$$C_n = [C_\ell \quad C_{n-\ell}]$$

and using (A_ℓ , B_ℓ , C_ℓ) as a truncated model. Note that the dimension of D_ℓ directly determines the dimension of A_ℓ , and hence, the order of the state-space model [see Eqs. (11)].

When a continuous (infinite-order) system such as a physical structure is being identified, it is necessary to make an engineering decision on which (and how many) states to retain. Typically, many states are weakly represented in the data and, if chosen carefully, can be truncated without having a large effect on the identified model's response. If the truncated states are chosen inappropriately, however, the performance of the reduced model can be degraded significantly. The method of model truncation in the ERA is to truncate states with small singular values ($D_{n-\ell}$), as described above. In the examples that follow, a state will be considered negligible if its singular value is less than 1/100 the size of the largest singular value. It will be shown that if the dimensions of $H_{rs}(0)$ are small, a better truncation criterion can sometimes be found.

The ERA has been used with both simulated and actual experimental data, and it has been shown to be an effective approach.^{1,8,9} Three important factors affect the accuracy of the state-space model produced by the ERA: 1) noise in the measurement data that leads to errors in the Markov parameters; 2) the size and content of $H_{rs}(0)$, i.e., the choice of r , s , t_i , and j_j ; and 3) the dimension of D_ℓ and $D_{n-\ell}$, the retained and truncated portions of D . In this paper it is assumed that the Markov parameters are accurately known so that no significant errors are introduced by item 1 in this list. It is then shown how the accuracy of the truncated model can be improved significantly without increasing the size of $H_{rs}(0)$ or D_ℓ .

Example of the Standard ERA

Before presenting the modified procedure that is the subject of this paper, we consider a simple example that illustrates how the choice of r , s , and the size of D_ℓ influences the accuracy of the resulting state-space model. For illustration, the simple discretized model of a bar in axial motion shown in Fig. 1 is used. In general, the time domain motion of a physical structure can be described by the second-order differential equation

$$M\ddot{x} + F\dot{x} + Kx = f \quad (13)$$

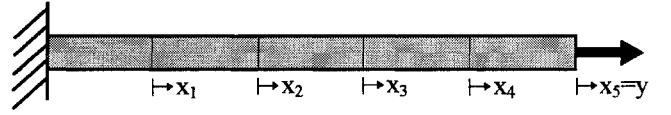


Fig. 1 Discretized bar model.

where x is the deformation vector, M is the mass matrix, F is a viscous damping matrix, K is the stiffness matrix, and f is the applied force vector. Equivalently, the dynamics can be represented by the first-order equation

$$\begin{Bmatrix} \dot{x} \\ \dot{\dot{x}} \end{Bmatrix} = \begin{bmatrix} 0 & I \\ -M^{-1}K & -M^{-1}F \end{bmatrix} \begin{Bmatrix} x \\ \dot{x} \end{Bmatrix} + \begin{Bmatrix} 0 \\ f \end{Bmatrix} \quad (14)$$

The bar is modeled using five linear finite elements with unit non-dimensional geometric and material properties ($A = \Delta L = E = \rho = 1.0$), leading to the following mass and stiffness matrices:

$$M = \begin{bmatrix} 1 & 0 & 0 & 0 & 0 \\ 0 & 1 & 0 & 0 & 0 \\ 0 & 0 & 1 & 0 & 0 \\ 0 & 0 & 0 & 1 & 0 \\ 0 & 0 & 0 & 0 & 0.5 \end{bmatrix}$$

$$K = \begin{bmatrix} 2 & -1 & 0 & 0 & 0 \\ -1 & 2 & -1 & 0 & 0 \\ 0 & -1 & 2 & -1 & 0 \\ 0 & 0 & -1 & 2 & -1 \\ 0 & 0 & 0 & -1 & 1 \end{bmatrix}$$

The damping matrix is assumed to be proportional to the stiffness matrix: $F = 0.005 \times K$. The time step for discretization is $\Delta t = 0.15$. The discrete-time system matrices A , B , and C are given by

$$A = \exp \left(\Delta t \begin{bmatrix} 0 & I \\ -M^{-1}K & -M^{-1}F \end{bmatrix} \right)$$

$$B = A[0 \quad 0 \quad 0 \quad 0 \quad 0 \quad 0 \quad 0 \quad 0 \quad 0 \quad 1]^T \quad (15)$$

$$C = [0 \quad 0 \quad 0 \quad 0 \quad 1 \quad 0 \quad 0 \quad 0 \quad 0 \quad 0]$$

This system has five natural modes, with discrete-time eigenvalues of $0.9998 \pm 0.0469i$, $0.9904 \pm 0.1357i$, $0.9769 \pm 0.2104i$, $0.9633 \pm 0.2638i$, and $0.9550 \pm 0.2916i$, corresponding to periods of 134, 46, 30, 24, and 21 time steps, respectively.

Consider first the case in which a very limited amount of data is available and a state-space realization is to be constructed using $r = s = 20$. Using $t_i = j_j = i$, the first 40 Markov parameters, representing approximately $\frac{1}{3}$ of a cycle of the dominant mode and almost a full cycle of the second mode of the system, are required in the construction of A , B , and C . In this case, the first few singular values of the Hankel matrix are

$$\text{diag}(D) = \begin{Bmatrix} 1.5055 \\ 0.2593 \\ 0.2584 \\ 0.0245 \\ 0.0014 \\ 0.0000 \\ 0.0000 \\ 0.0000 \\ \vdots \end{Bmatrix}$$

If the Hankel matrix singular values are the only indicators used to determine the required order of the realized model using the criterion described above, a fourth-order model containing only the first

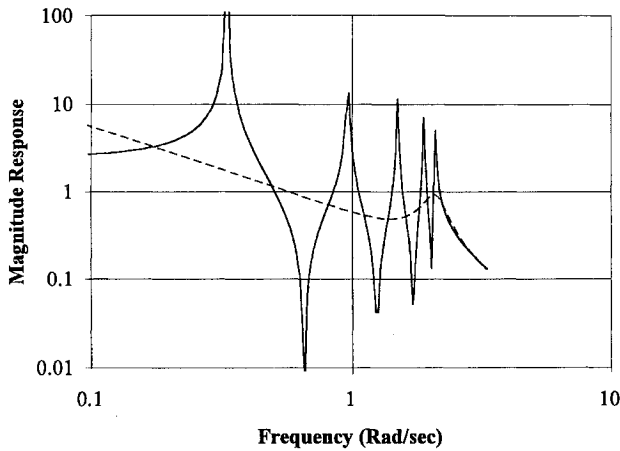


Fig. 2 Magnitude frequency response: —, model $M_{10,\infty}$ (true model) and ---, model $M_{4,40}$.

four states would be expected to perform very well. This model will be referred to as $M_{4,40}$. The first subscript indicates the order of the model, and the second subscript indicates the number of Markov parameters used to construct the model. The frequency response of model $M_{4,40}$ is plotted in Fig. 2, along with the exact 10th-order system response (model $M_{10,\infty}$). Indeed, model $M_{4,40}$ is an extremely good approximation at high frequencies (the frequencies most visible in the limited data window), but the low-frequency performance misses the largest peaks in the frequency response. The eigenvalues of this model are 0.9970, 0.7582, and $0.9292 \pm 0.2828i$. Note that model $M_{4,40}$ has nonoscillatory eigenvalues, which do not exist in the physical system.

Consider now a case in which a large amount of data is available, $r = s = 1000$. The construction of A , B , and C requires the first 2000 Markov parameters, representing many cycles of each mode of the system. In this case, the first few singular values of $H_{r,s}(0)$ are

$$\text{diag}(D) = \begin{Bmatrix} 46.3003 \\ 46.1442 \\ 12.3867 \\ 12.2322 \\ 5.5083 \\ 5.4491 \\ 3.1968 \\ 3.1664 \\ 2.4427 \\ 2.4185 \\ 0 \\ \vdots \end{Bmatrix}$$

Here, there are measurable contributions from the first 10 states (as expected for a 10th-order system), but only the first six appear to be important. Therefore, we decide that a sixth-order model (model $M_{6,2000}$) will be constructed. The frequency response of model $M_{6,2000}$ is plotted in Fig. 3, along with the frequency response of model $M_{10,\infty}$. The eigenvalues of this model are $0.9989 \pm 0.0469i$, $0.9904 \pm 0.1357i$, and $0.9769 \pm 0.2103i$, which are essentially identical to the three lowest-frequency eigenvalues of the physical system. Model $M_{6,2000}$ provides a much better approximation than model $M_{4,40}$.

Because a sixth-order model (model $M_{6,2000}$) has been shown to work well, the reader's first reaction might be to go back to $r = s = 20$ and construct a sixth-order model based on the first 40 Markov parameters (model $M_{6,40}$). The frequency response of model $M_{6,40}$ is plotted against model $M_{10,\infty}$ in Fig. 4, and the eigenvalues of the model are 0.9963, 0.8841, $0.9477 \pm 0.2855i$, and $0.9064 \pm 0.2000i$. The performance is only slightly better than that of the fourth-order model.

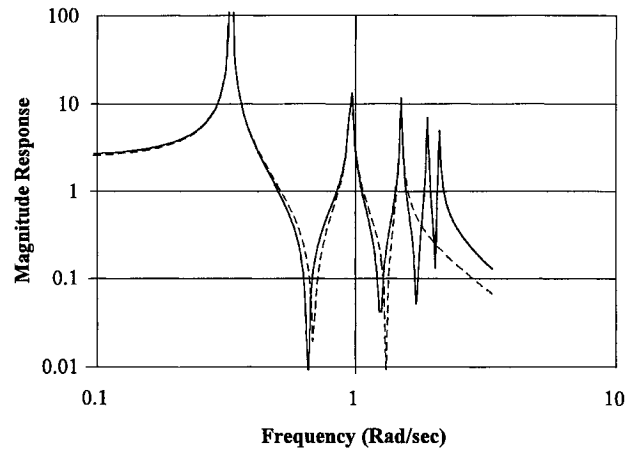


Fig. 3 Magnitude frequency response: —, model $M_{10,\infty}$ (true model) and ---, model $M_{6,2000}$.

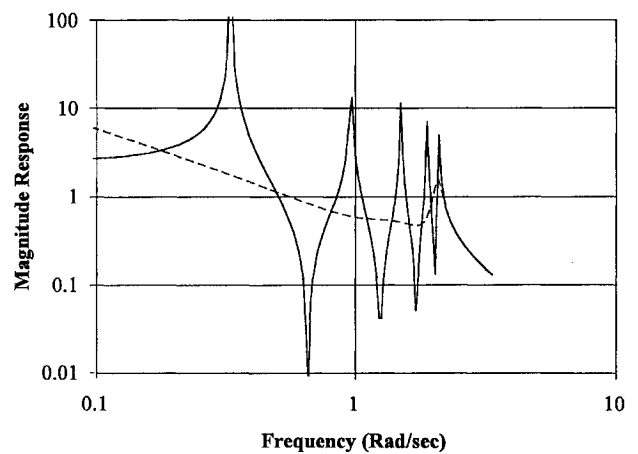


Fig. 4 Magnitude frequency response: —, model $M_{10,\infty}$ (true model) and ---, model $M_{6,40}$.

Rebalancing

To shed some light on why the singular values of the generalized Hankel matrix can be unreliable indicators of the relative importance of states when short data records are used and to motivate the development of a procedure with better performance, we define the finite-time generalized controllability and observability gramians as

$$\begin{aligned} W_{\ell,s}^C &= \sum_{k=0}^{s-1} A_\ell^{jk} B_\ell B_\ell^T (A_\ell^T)^{jk} \\ W_{\ell,r}^O &= \sum_{k=0}^{r-1} (A_\ell^T)^{jk} C_\ell^T C_\ell A_\ell^{jk} \end{aligned} \quad (16)$$

The definitions of $W_{\ell,s}^C$ and $W_{\ell,r}^O$ are more general than the usual definition of controllability and observability gramians. $W_{\ell,s}^C$ and $W_{\ell,r}^O$ reduce to the more conventional controllability and observability gramians when $j_i = i$ and $t_i = i$. If an untruncated triple (A_n, B_n, C_n) obtained using the ERA is used to formulate $W_{n,s}^C$ and $W_{n,r}^O$, then it can be shown that

$$W_{n,s}^C = W_{n,r}^O = D \quad (17)$$

where D is the diagonal matrix of singular values in Eq. (8).

When the generalized controllability and observability gramians are equal and diagonal, the realization is said to be internally balanced. Internally balanced models have been studied by a number of researchers, and they have been shown to possess some useful properties.¹⁰ In most cases, however, these studies focus on stable

models that are balanced with respect to infinite-time controllability and observability gramians defined as

$$\mathbf{W}_{n,\infty}^C = \sum_{k=0}^{\infty} \mathbf{A}_n^k \mathbf{B}_n \mathbf{B}_n^T (\mathbf{A}_n^T)^k \quad \mathbf{W}_{n,\infty}^O = \sum_{k=0}^{\infty} (\mathbf{A}_n^T)^k \mathbf{C}_n^T \mathbf{C}_n \mathbf{A}_n^k \quad (18)$$

Models that are balanced with respect to $\mathbf{W}_{n,s}^C$ and $\mathbf{W}_{n,r}^O$ may not possess the useful properties of those balanced with respect to $\mathbf{W}_{n,\infty}^C$ and $\mathbf{W}_{n,\infty}^O$. One way to approximate infinite-time balancing is to let $j_i = i$ and $t_i = i$ and let r and s get very large, as in creating model $\mathbf{M}_{4,2000}$. The difficulty with this is that the Hankel matrices $\mathbf{H}_{rs}(0)$ and $\mathbf{H}_{rs}(1)$ get very large and they require a large number of Markov parameters for their construction and a large computational effort for their decomposition. Fortunately, there is an alternative, which is to perform a transformation on the state-space model before the truncation is performed. The modified procedure is as follows.

First, $\mathbf{H}_{rs}(0)$ is formed and decomposed as described earlier [Eq. (8)]. The minimum size of $\mathbf{H}_{rs}(0)$ depends on the uncertainty (noise) in the Markov parameters and the order of the model. For the noise-free single-input, single-output case, the minimum required number of Markov parameters is twice the order of the system. Using \mathbf{P} , \mathbf{D} , and \mathbf{Q} , form the largest possible state matrices $(\mathbf{A}_n, \mathbf{B}_n, \mathbf{C}_n)$, where $n = \text{rank}[\mathbf{H}_{rs}(0)]$. The system described by this model is internally balanced with respect to the finite-time controllability and observability gramians. With a change of variables, a model can be produced that is internally balanced with respect to the infinite-time gramians and that offers improved performance when truncated. Consider a transformation of the form

$$\tilde{\mathbf{x}} = \mathbf{T}^{-1} \mathbf{x} \quad (19)$$

The state matrices in the transformed coordinates can be expressed as

$$\tilde{\mathbf{A}} = \mathbf{T}^{-1} \mathbf{A} \mathbf{T} \quad \tilde{\mathbf{B}} = \mathbf{T}^{-1} \mathbf{B} \quad \tilde{\mathbf{C}} = \mathbf{C} \mathbf{T} \quad (20)$$

Substituting the new state matrices into Eqs. (18), it can easily be seen that the infinite-time controllability and observability gramians for the transformed coordinates are related to those in the original coordinates by the relationships

$$\tilde{\mathbf{W}}_{n,\infty}^C = \mathbf{T}^{-1} \mathbf{W}_{n,\infty}^C \mathbf{T}^{-T} \quad \tilde{\mathbf{W}}_{n,\infty}^O = \mathbf{T}^T \mathbf{W}_{n,\infty}^O \mathbf{T} \quad (21)$$

The transformation matrix \mathbf{T} that produces a system that is balanced with respect to the infinite-time controllability and observability gramians can be efficiently computed from the Cholesky factors of the infinite-time gramians.^{11,12} The infinite-time gramians in the rebalanced coordinates are

$$\tilde{\mathbf{W}}_{n,\infty}^C = \tilde{\mathbf{W}}_{n,\infty}^O = \tilde{\mathbf{W}} = \begin{bmatrix} \ddots & & \\ & w_i & \\ & & \ddots \end{bmatrix} \quad (22)$$

The w_i can then be used as measures of the relative importance of the various states but are free of the bias toward the data sample interval reflected in the singular values of $\mathbf{H}_{rs}(0)$. The gramians and the state matrices can be partitioned as

$$\tilde{\mathbf{W}} = \begin{bmatrix} \tilde{\mathbf{W}}_\ell & \\ & \tilde{\mathbf{W}}_{n-\ell} \end{bmatrix} \quad \tilde{\mathbf{A}} = \begin{bmatrix} \tilde{\mathbf{A}}_\ell & \tilde{\mathbf{A}}_{\ell,n-\ell} \\ \tilde{\mathbf{A}}_{n-\ell,\ell} & \tilde{\mathbf{A}}_{n-\ell} \end{bmatrix} \quad (23)$$

$$\tilde{\mathbf{B}} = \begin{bmatrix} \tilde{\mathbf{B}}_\ell \\ \tilde{\mathbf{B}}_{n-\ell} \end{bmatrix} \quad \tilde{\mathbf{C}} = [\tilde{\mathbf{C}}_\ell \quad \tilde{\mathbf{C}}_{n-\ell}]$$

If the elements of $\tilde{\mathbf{W}}_\ell$ are large compared to the elements of $\tilde{\mathbf{W}}_{n-\ell}$, the system can be approximated by the triple $(\tilde{\mathbf{A}}_\ell, \tilde{\mathbf{B}}_\ell, \tilde{\mathbf{C}}_\ell)$. Note the similarity to Eqs. (12).

Within the context of the ERA, the new procedure can be summarized as follows:

1) Choose appropriate values for r , s , t_i , and j_i . The choices of r and s must be large enough to accurately identify untruncated system matrices of sufficient order. This required size is much smaller

than that required to produce accurate reduced-order models without rebalancing.

2) Form the generalized Hankel matrices $\mathbf{H}_{rs}(0)$ and $\mathbf{H}_{rs}(1)$ [Eq. (5)].

3) Using the singular-value decomposition, decompose $\mathbf{H}_{rs}(0)$ [Eq. (8)].

4) Form the largest possible system matrices \mathbf{A}_n , \mathbf{B}_n , and \mathbf{C}_n [Eqs. (11)].

5) Compute the infinite-time controllability and observability gramians $\mathbf{W}_{n,\infty}^C$ and $\mathbf{W}_{n,\infty}^O$ [Eqs. (18)].

6) Compute the transformation \mathbf{T} and the diagonal infinite-time gramian $\tilde{\mathbf{W}}$, and transform \mathbf{A}_n , \mathbf{B}_n , and \mathbf{C}_n into their balanced counterparts $\tilde{\mathbf{A}}_n$, $\tilde{\mathbf{B}}_n$, and $\tilde{\mathbf{C}}_n$ [Eqs. (20)].

7) Truncate the rebalanced system matrices based on the diagonal elements of $\tilde{\mathbf{W}}$.

The following example illustrates the performance improvement that can be realized in the identified model using the new procedure.

Example of Rebalancing

To illustrate the improvement provided by this procedure, consider again the problem of modeling the discretized bar model using the first 40 Markov parameters ($r = s = 20$). After forming a 10th-order model and performing the rebalancing transformation, the first few diagonal elements of $\tilde{\mathbf{W}}_\infty$ are

$$\text{diag}(\tilde{\mathbf{W}}_\infty) = \begin{bmatrix} 653.5073 \\ 652.4857 \\ 26.7607 \\ 26.6392 \\ 7.0810 \\ 7.0306 \\ 3.5279 \\ 3.4948 \\ 2.5843 \\ 2.5609 \\ 0 \\ 0 \end{bmatrix}$$

Because the system is 10th order and there is no noise, $\text{rank } \mathbf{H}_{rs}(0)$ is 10, even though $\mathbf{H}_{rs}(0)$ is 20×20 . The first six states appear to be important (as expected from the results of the case in which $r = s = 1000$). Retaining the most important states, a sixth-order model (model $\tilde{\mathbf{M}}_{6,40}$) was constructed, and the frequency response is plotted against model $\mathbf{M}_{10,\infty}$ in Fig. 5. The eigenvalues of this model are $0.9989 \pm 0.0469i$, $0.9904 \pm 0.1357i$, and $0.9769 \pm 0.2103i$, which are essentially identical to the three lowest-frequency eigenvalues of the physical system and to the eigenvalues of model $\mathbf{M}_{6,2000}$. Model $\tilde{\mathbf{M}}_{6,40}$ proves to be very accurate, surpassing even model $\mathbf{M}_{6,2000}$.

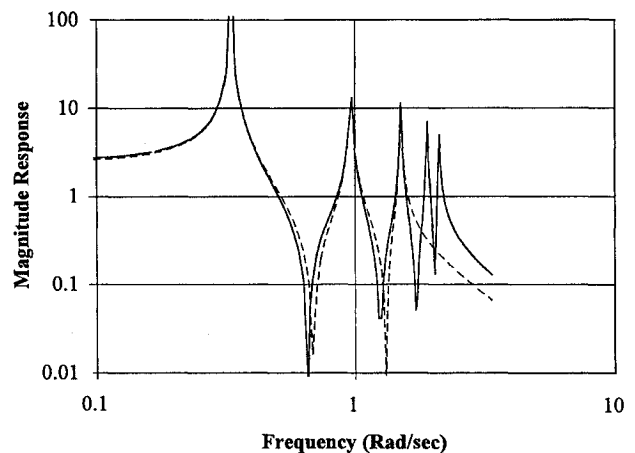


Fig. 5 Magnitude frequency response: —, model $\mathbf{M}_{10,\infty}$ (true model) and ---, model $\tilde{\mathbf{M}}_{6,40}$.

Conclusion

In off-line system identification algorithms, one of the most important problems is determining how many states are important to the input-output relationship of the system (the order of the identified model). Some current system identification techniques, such as the ERA, base the selection of important states on the relative magnitudes of the singular values of a generalized Hankel matrix. This results in state-space models that are internally balanced with respect to finite-time controllability and observability gramians, which are implicitly defined by the Markov parameters used to form the generalized Hankel matrix. If the order of the identified model is lower than the order of the physical system, unimportant states (states corresponding to small singular values of the generalized Hankel matrix) are neglected. If the amount of pulse-response data used in the procedure is insufficient, the criterion used to determine the model order and select the unimportant states can become unreliable and the truncation step can introduce significant errors into the identified model. It has been shown that truncating models that are balanced with respect to infinite-time gramians can produce results superior to those of truncating models that are balanced with respect to the implicitly defined finite-time gramians. This observation can be applied directly to the ERA, resulting in changes to the criterion for selecting model order and a modified definition of the identified system matrices. This removes an implicit bias toward the time interval represented by the pulse response data and can dramatically improve the fidelity of a reduced-order identified model when a limited amount of response data is available.

References

¹Juang, J. N., and Pappa, R. S., "An Eigensystem Realization Algorithm for Modal Parameter Identification and Model Reduction," *Journal of Guid-*

ance, Control, and Dynamics, Vol. 8, No. 5, 1985, pp. 620-627.

²Juang, J. N., *Applied System Identification*, Prentice-Hall, Englewood Cliffs, NJ, 1994, Chap. 5.

³Ljung, L., *System Identification: Theory for the User*, Prentice-Hall, Englewood Cliffs, NJ, 1987.

⁴Ho, B. L., and Kalman, R. E., "Effective Construction of Linear State Variable Models from Input/Output Data," *Proceedings of the 3rd Annual Allerton Conference on Circuit and System Theory*, 1965, pp. 449-459; also "Effective Construction of Linear State-Variable Models from Input/Output Functions," *Regelungstechnik*, Vol. 14, 1966, pp. 545-548.

⁵Juang, J. N., Phan, M., Horta, L. G., and Longman, R. W., "Identification of Observer/Kalman Filter Markov Parameters: Theory and Experiments," *Journal of Guidance, Control, and Dynamics*, Vol. 16, No. 2, 1993, pp. 320-329.

⁶Press, W. H., et al., *Numerical Recipes in C: The Art of Scientific Computing*, Cambridge Univ. Press, Cambridge, England, UK, 1988.

⁷Klema, V. C., and Laub, A. J., "The Singular Value Decomposition: Its Computation and Some Applications," *IEEE Transactions on Automatic Control*, Vol. AC-25, No. 2, 1980, pp. 164-176.

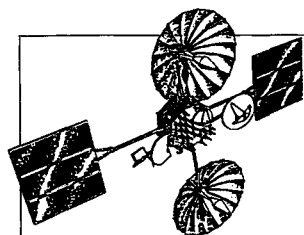
⁸Juang, J. N., and Pappa, R. S., "Effects of Noise on Modal Parameters Identified by the Eigensystem Realization Algorithm," *Journal of Guidance, Control, and Dynamics*, Vol. 9, No. 3, 1986, pp. 294-303.

⁹Pappa, R. S., and Juang, J. N., "Some Experiences with the Eigensystem Realization Algorithm," *Journal of Sound and Vibration*, Vol. 22, No. 1, 1988, pp. 30-35.

¹⁰Moore, B. C., "Principal Component Analysis in Linear Systems: Controllability, Observability, and Model Reduction," *IEEE Transactions on Automatic Control*, Vol. AC-26, No. 1, 1981, pp. 17-31.

¹¹Horta, L. G., Juang, J. N., and Longman, R. W., "Discrete-Time Model Reduction in Limited Frequency Ranges," *Journal of Guidance, Control, and Dynamics*, Vol. 16, No. 6, 1993, pp. 1125-1130.

¹²Laub, A. J., Heath, M. T., Paige, C. C., and Ward, R. C., "Computation of System Balancing Transformations and Other Applications of Simultaneous Diagonalization Algorithms," *IEEE Transactions on Automatic Control*, Vol. AC-32, No. 2, 1987, pp. 115-122.



Satellite Thermal Control Handbook

David G. Gilmore, *editor*

The new *Satellite Thermal Control Handbook* (David G. Gilmore, Editor), published by The Aerospace Corporation Press and distributed by AIAA, is a compendium of corporate knowledge and heritage of thermal control of unmanned Earth-orbiting satellites. This practical handbook provides thermal engineers of all experience levels with enough background and specific information to begin conducting thermal analysis and to participate in the thermal design of satellite systems.

1994, 581 pp, illus, Paperback, ISBN 1-8849889-00-4, Order #: 00-4(945), AIAA Members: \$59.95, Nonmembers: \$79.95

Contents:

Satellite Systems Overview
Satellite Configurations
Orbits
Missions
Satellite Thermal Environments
Types of Environmental Loads
Environments in Typical Orbits
Launch/Ascent Environment
Thermal Design Examples
Spin-Stabilized Satellites
3-Axis-Stabilized Satellites
Propulsion Systems
Batteries
Antennas
Sun/Earth/Star Sensors
Cooled Devices
Solar Arrays
Systems Overview—The Hubble Space Telescope

Thermal Control Hardware
Section 1: Thermal Surface Finishes
Section 2: Mounting and Interfaces
Section 3: Multilayer Insulation and Barriers
Section 4: Heaters, Thermostats, and Solid State Controllers
Section 5: Louvers
Section 6: Radiators
Section 7: Thermoelectric Coolers
Section 8: PCMs and Heat Sinks
Section 9: Pumped Fluid Loops
Thermal Design Analysis
Satellite Project Phases
Thermal Design/Analysis Process Overview
Fundamentals of Thermal Modeling
Thermal Design Analysis Example—POAM Margins

Thermal Math Model Computer Codes (SINDA)
Space Shuttle Integration
Engineering Compatibility
The Cargo Integration Review Safety
Heat Pipes and Capillary Pumped Loops
Why a Heat Pipe Works
Constant-Conductance Heat Pipes
Diode Heat Pipes
Variable-Conductance Heat Pipes
Capillary Pumped Loops
Hybrid (Mechanically Assisted) Systems
Analysis
Materials
Compatibility
Testing
Heat Pipe Applications/Performance

Cryogenic Systems
Stored-Cryogenic Cooling Systems
Cryogenic Radiators
Refrigerators
Design and Test Margins for Cryogenic Systems
Thermal Testing
Design Environments
Component Testing
Developmental and Subsystem Thermal Testing
Space Vehicle Thermal Tests
Factory and Launch-Site Thermal Testing
Test Techniques
Testing Checklist
One-of-a-Kind Spacecraft Thermal Testing
Technology Projections
Appendices

Place your order today! Call 1-800/682-AIAA



American Institute of Aeronautics and Astronautics

Publications Customer Service, 9 Jay Gould Ct., P.O. Box 753, Waldorf, MD 20604
FAX 301/843-0159 Phone 1-800/682-2422 8 a.m. - 5 p.m. Eastern

Sales Tax: CA residents, 8.25%; DC, 6%. For shipping and handling add \$4.75 for 1-4 books (call for rates for higher quantities). Orders under \$100.00 must be prepaid. Foreign orders must be prepaid and include a \$25.00 postal surcharge. Please allow 4 weeks for delivery. Prices are subject to change without notice. Returns will be accepted within 30 days. Non-U.S. residents are responsible for payment of any taxes required by their government.